Chemical diffusion of oxygen in single-crystal and polycrystalline $YBa_2Cu_3O_{6+x}$ determined by electrical-resistance measurements

John R. LaGraff and David A. Payne
Department of Materials Science and Engineering and Materials Research Laboratory, University of Illinois at Urbana-Champaign, Urbana, Illinois 61801
(Received 7 February 1992; revised manuscript received 24 June 1992)

Isothermal electrical-resistance measurements were used to monitor oxygen diffusion kinetics in both single-crystal and polycrystalline $YBa_2Cu_3O_{6+x}$ between 350 and 780 °C. Distinctions are made between intrinsic diffusion behavior and microstructure-dependent properties. An activation energy of 0.4(1) eV was determined for oxygen in-diffusion in dense polycrystalline material from 400 to 780 °C, and 1.10(6) eV for single crystals between 600 and 780 °C. Below 600 °C, the activation energies for out-diffusion in porous and dense polycrystalline specimens were determined to be 0.5(1) eV and 0.6(1) eV, respectively. The lower activation energy in polycrystalline specimens was attributed to (i) shell effects at either grain boundaries or the specimen surface in which the rapid formation of a highly oxygenated skin created short-circuit pathways for current flow, and (ii) high-diffusivity pathways along grain boundaries. Measurements on single crystals reveal that the intrinsic rate of oxygen in-diffusion was comparable to, if not slower, than out-diffusion, which was contrary to measurements on polycrystalline specimens. This type of behavior was attributed to the formation of a highly oxygenated shell during in-diffusion which behaved as both (i) a high-conductivity pathway and (ii) a barrier to bulk oxygen in-diffusion. The use of single crystals enabled these effects to be clearly distinguished.

I. INTRODUCTION

Oxygen stoichiometry has a profound effect on the superconducting, normal state, and structural properties of $YBa_2Cu_3O_{6+x}$ (YBCO).[1,2] Consequently, an understanding of the chemical diffusion of oxygen $\tilde{D}$ is important for the processing of YBCO with specific property requirements in all of its requisite forms (e.g., bulk, melt-textured, single-crystal, thin-film, wire, etc.). Fundamental oxygen diffusion behavior has been reported by tracer-diffusion techniques[3–5] and internal friction measurements,[6–9] however, it is the chemical diffusion of oxygen, under a concentration gradient, which is most important for the processing of YBCO. The oxygen chemical diffusion coefficient is measured under a gradient in the chemical potential, which is most often achieved through changes in oxygen partial pressure surrounding the specimen, or changes in temperature. $\tilde{D}$ is related to the tracer or self-diffusivity D^* by the equation[10]

$$\tilde{D}=D^*\left[1+\frac{\partial \ln\gamma}{\partial \ln c}\right], \tag{1}$$

where the term in brackets is the thermodynamic enhancement factor containing the solute activity γ and concentration c of the diffusing species. In an ideal solution (often in the dilute limit), the activity γ is unity for all concentrations and the tracer-diffusion and chemical diffusion coefficients are equal. In the YBCO system, however, a significant contribution of the thermodynamic factor [Eq. (1)] is expected from studies of oxygen partial pressure as a function of oxygen concentration.[11,12] These results explain why values of $\tilde{D}$ reported for YBCO have generally been greater than the tracer or self-diffusivities.

The two most common techniques used to measure $\tilde{D}$ in YBCO are electrical-resistance measurements,[13–31] and thermogravimetric analysis,[12,30,32–36] which monitor the electron-hole content and mass, respectively, associated with oxygen exchange. Other techniques include solid-state electrochemical measurements,[37–41] gas volumetry,[42,43] *in situ* neutron diffraction,[43,44] differential scanning calorimetry,[45] IR spectroscopy,[35] and positron annihilation.[46] The remarkable agreement found in the tracer- and self-diffusivity studies[3–9] with regards to diffusion coefficients and activation energies is unfortunately lacking in the chemical diffusion studies.[13–46] In addition to the more complex situation for chemical diffusion (e.g., solute activities), these discrepancies can be attributed to different sample microstructures and experimental techniques.

In this paper, we report electrical-resistance measurements of oxygen diffusion kinetics in single-crystal and polycrystalline YBCO. A particular advantage of the electrical-resistance method, in addition to its extreme sensitivity to small changes in oxygen content, Δx, is the ability to make repeated measurements on a single specimen. This ensures high reproducibility by removing sample-to-sample variance, which enables subtle changes in oxygen diffusion behavior to be more readily distinguished. All of these factors make resistance measurements especially suitable for monitoring diffusion kinetics in single crystals of YBCO whose small mass precludes the use of thermogravimetric analysis. However, one is measuring a response that is attributed to the dynamic change in the carrier concentration and associated scattering processes and, thus, assumptions must be made

on the relationships between oxygen content, electron-hole concentration, and the overall resistance of the specimen.

YBCO is principally an electronic conductor with extremely low oxygen anion transference numbers (10^{-9} to 10^{-7} in Refs. 23 and 37). The electrical conductivity σ for majority hole carriers can be written as

$$\sigma=[h^{\cdot}]\mu e \ , \tag{2}$$

where $[h^{\cdot}]$ is the hole concentration, μ is the hole mobility, and e is the electron charge. Isothermal measurements allow the mobility term to be neglected and thus an increase in the resistance is largely a consequence of a decrease in the hole concentration as oxygen leaves the system according to the defect relation[14,23]

$$O_O^x+2h^{\cdot}\rightleftarrows V_O^{\cdot\cdot}+\tfrac{1}{2}O_2 \ , \tag{3}$$

where $V_O^{\cdot\cdot}$ denotes a doubly ionized (positive) vacant O(1) chain oxygen site, and O_O^x is the neutral occupied O(1) site. Defect models in a highly defective and nonstoichiometric compound such as YBCO are expected to be more complex. Theoretically, Eq. (3) describes a dilute solution of noninteracting oxygen anions and should be regarded as a first approximation of the relationship between the majority carriers and the oxygen content in YBCO.

Resistance measurements require that assumptions be made concerning the actual distribution of oxygen within the specimen, i.e., a diffusion mechanism must be assumed. The change in resistance with time $\Delta R(t)$ of YBCO is proportional to the change in oxygen content $\Delta x(t)$ according to the relation

$$\left[\frac{\ln R(t)-\ln R(0)}{\ln R(\infty)-\ln R(0)}\right]\equiv\left[\frac{x(t)-x(0)}{x(\infty)-x(0)}\right]\equiv\alpha(t) \ , \tag{4}$$

where $R(0)$ is the resistance at the beginning of in- or out-diffusion, $R(t)$ the resistance as a function of time, $R(\infty)$ the eventual saturation resistance, and $\alpha(t)$ the fractional change in resistance (or oxygen content). The resistance change during oxygen diffusion in rectangular bars of polycrystalline YBCO can be fit to the equation for one-dimensional diffusion into a plane[47]

$$\alpha(t)=1-\frac{8}{\pi^2}\sum_{n=0}^{\infty}\frac{1}{(2n+1)^2}\exp\left[\frac{-(2n+1)^2t}{\tau}\right] \ , \tag{5}$$

where the relaxation time τ is related to the chemical diffusivity $\tilde{D}$ by the expression

$$\tilde{D}=\frac{L^2}{\pi^2\tau} \ , \tag{6}$$

and L is the effective diffusion length. The large anisotropy in the tracer diffusivities[5] of YBCO suggests that oxygen exchange in single crystals will occur primarily at the edges of the thin platelets (i.e., it will be a two-dimensional process). This in turn can be represented by the two-dimensional analogue of Eq. (5) in which the presummation term is replaced by $64/\pi^4$ and the effective diffusion length L in Eq. (6) is replaced by

$$L^2=(1/L_a^2+1/L_b^2)^{-1}$$

where L_a and L_b are the crystal dimensions in the ab plane.

It is evident that, in addition to the measurement of accurate relaxation times, one must also choose an appropriate effective diffusion length L to estimate reliable diffusivities [Eq. (6)]. Unfortunately, this is often the most difficult step in interpreting the results of chemical diffusion studies especially in YBCO. Not only does the effective diffusion length depend on microstructural features such as grain size and connected porosity, but quite possibly on the experimental technique. For example, heterogeneous oxygen distributions may lead to shell effects, especially during in-diffusion. These shells may behave as short-circuit pathways for electrical current thus yielding resistances that are not representative of the bulk oxygen content.[27,28,30] With these motivations in mind, a study of the chemical diffusion behavior in both single-crystal and polycrystalline YBCO was undertaken to distinguish between intrinsic oxygen diffusion rates, and those influenced—if not dominated—by such factors as grain size, bulk density, and short-circuit pathways for current flow, which can occur in polycrystalline ceramic superconductors.

II. EXPERIMENTAL

A. Sample preparation

The authors have experience in the growth of doped and undoped single crystals of YBCO and have prepared and measured over 30 batches. Large single crystals of various sizes (up to $10\times10\times2$ mm^3) were grown in either alumina or yttria-stabilized zirconia crucibles by a standard self-flux technique described elsewhere.[13] Resistance measurements were made on many of these crystals during oxygen diffusion, and the results were found to be consistent from crystal to crystal, and from batch to batch.[13–18] The authors report here extensive resistance

TABLE I. Data for single crystals and polycrystalline YBCO specimens.

Specimen type	T_c	Specimen size (mm^3)	Grain size (mm)	Bulk density
Crystal $C1$	90 K	$1\times1\times0.05$		
Crystal $C2$	90 K	$2\times1.5\times0.5$		
Polycrystal $S1$	92 K	$4.85\times2.05\times0.50$	$1.1(2)\times6(1)$	75(5)%
Polycrystal $S2$	92 K	$4.70\times1.55\times0.90$	$2.8(4)\times19(3)$	95(5)%

measurements on two representative crystals, which serve to illustrate the general observations. The two twinned crystals had dimensions of approximately $1\times1\times0.05$ and $2\times1.5\times0.5$ mm^3 (hereafter referred to as $C1$ and $C2$, respectively) with the c axis oriented in the thin direction (Table I). The critical temperatures, T_c (onset), from superconducting quantum interference device (SQUID) susceptibility measurements were 90 K for both crystals with a transition width (10–90%) of 1 K.

YBCO powder was prepared by a standard mixed-oxide route as described previously.[48] Polycrystalline specimens of different grain sizes and bulk densities were obtained by pressing pellets at 24 MPa and then sintering for 24 h in oxygen at temperatures from 950 to 980 °C. We report here data on the two extremes in bulk densities as means of illustrating the influence of microstructure on the oxygen diffusion behavior as measured by the electrical resistance method. The bulk densities of specimens #1 ($S1$) and #2 ($S2$) were ~75(5) and ~95(5) %, respectively. The acicular grains had average dimensions of ~1.1(2)×6(1) and ~2.8(4)×19(3) μm for specimens $S1$ (porous) and $S2$ (dense), respectively (Fig. 1, Table I). Following a one week anneal at 500 °C in oxygen, x-ray analysis (scan rate, 1° 2θ/min; Cu $K\alpha$ radiation, 20 mA and 45 mV) indicated that the polycrystalline specimens were "phase-pure" and orthorhombic. SQUID susceptibility measurements yielded broad transitions (<2 K) with onset critical temperatures of 92 K. The pellets were subsequently sectioned into rectangular bars and polished to a 1 μm finish prior to resistance measurements. At least two bars were measured from each pellet and consistent results were obtained.

B. Electrical-resistance measurements

Measurements of electrical resistance during oxygen in-diffusion and out-diffusion were made by a computer-controlled four-point probe ac technique, while the specimen was simultaneously mounted in the hot stage of an optical microscope.[13,14] The applied ac current was kept constant at 1.86 mA (564 Hz) by a Stanford Research Systems SR530 lockin amplifier. Four gold wires (0.1% Be addition, 2 mil) were attached with silver paste to the corners of the (001) face of the single crystals and along the length of rectangular ceramic bars cut from the ceramic pellets. After annealing at 600° for several hours, the contacts had resistances of one ohm or less and had ohmic characteristics. Contact integrity was checked periodically throughout the measurements in both positive and negative dc currents. In order to further ascertain sample quality and contact integrity, resistivities were estimated from the geometry of polycrystalline specimens and by Montgomery's technique[49] for single crystals at various temperatures. The resistivities (ρ_{ab}) of the crystals were on the order of 100–200 $\mu\Omega$ cm at room temperature and 1–10 mΩ cm from 600–780 °C (100% oxygen). The bulk resistivities of the ceramic specimens were typically on the order of 3–30 mΩ cm from 350–780 °C. These values are in good agreement with those cited in the literature.[50]

Isothermal oxygen out-diffusion and in-diffusion was monitored by resistance measurements for single crystals

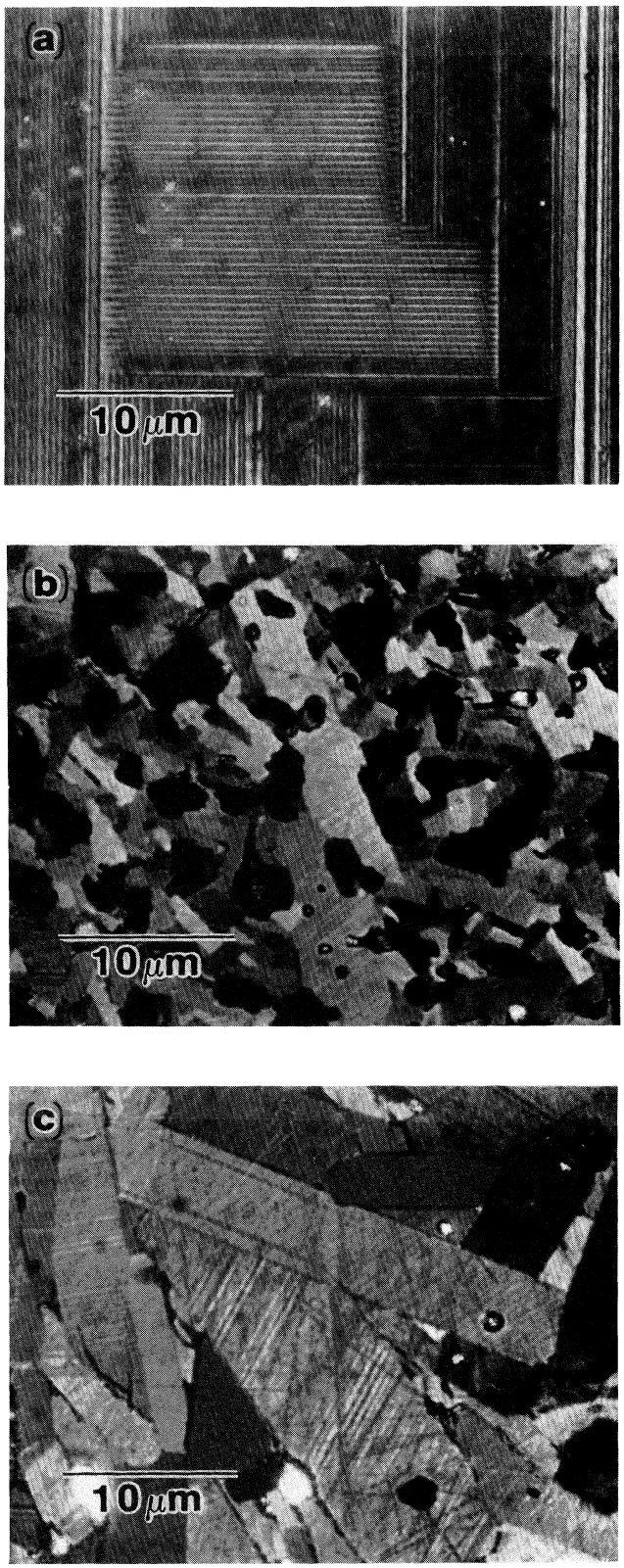

FIG. 1. Optical photomicrographs under cross-polarized reflected light of (a) single-crystal, (b) *porous*, fine-grain polycrystalline specimen $S1$, and (c) *dense*, coarse-grain polycrystalline specimen $S2$.

from 600–780 °C and for polycrystalline specimens from 350–780 °C. Resistance measurements in single crystals were prohibitively slow below 600 °C due to slow oxygen diffusion kinetics. (Several weeks are required to establish equilibrium in crystals.) The specimen was initially annealed in oxygen at the measurement temperature until equilibrium was established (> 36 h for crystals) as determined from calculations and by monitoring for constant resistance. Oxygen out-diffusion studies were carried out by introducing argon into the hot stage and recording the resistance increase of the specimen as a function of time. Following the argon anneal, oxygen was reintroduced into the system and the resistance decrease associated with oxygen in-diffusion was recorded. Water vapor and CO_2, which can degrade YBCO,[51] were removed from the ambient by a scrubbing column that contained CaO and $CaSO_4$. The strain accompanying the ferroelastic tetragonal-orthorhombic (TO) phase transformation was accommodated by the formation of {110} twin boundaries.[52] These transformation twins were clearly visible under polarized reflected light [see Fig. 1(a)] and enabled the phase transformation to be observed in an optical microscope during the resistance measurements.[13,14] Observation of the twin networks indicated that the crystal retained the orthorhombic structure below ~700 °C, and the tetragonal form above ~700 °C, when in equilibrium with pure oxygen. The crystal was driven isothermally through the orthorhombic-tetragonal (OT) transformation below ~700 °C by switching between oxygen and argon gases, however, no anomalies were observed in the measured resistance values.

III. RESULTS AND DISCUSSION

A. In-diffusion

Normalized resistance isotherms during oxygen in-diffusion for YBCO single crystals reveal a change in functional form as the temperature increased [e.g., crystal *C*2 in Fig. 2(a)]. Relaxation times during in-diffusion for crystals *C*1 and *C*2 were determined by fitting the data to the two-dimensional analogue of Eq. (5). An Arrhenius plot of the normalized relaxation times for crystals *C*1 and *C*2 yielded an activation energy for in-diffusion of 1.10(6) eV from 600–780 °C [Fig. 2(b)]. A similar analysis for dense polycrystalline material *S*2 yielded an activation energy of ~0.4(1) eV for in-diffusion from 400–780 °C [Fig. 2(c)]. (The rate of resistance change during in-diffusion for specimen *S*1 was too rapid for reliable determinations of relaxation time.) The activation energy (~0.4 eV) for in-diffusion from 400–780 °C in *dense,* large-grain specimen *S*2 [Fig. 2(c)] was similar to the values reported by Tu *et al.*[27] (~0.5 eV) from 210–360 °C and by Ottaviani *et al.*[28] (~0.4 eV) from 215–315 °C for the early stages of in-diffusion. These low values in comparison with single-crystal data (~1.10(6) eV) suggests either grain-boundary diffusion or the formation of a highly oxygenated conductive shell region,[27,28,30] the latter obscuring intrinsic in-diffusion behavior. Both Tu *et al.*[27] and Ottaviani *et al.*[28] measured in-diffusion activation energies of ~1.3 and 0.9 eV, respectively, for the latter stages of in-diffusion suggesting that the activation energy of ~1.10 eV for single crystals [Fig. 2(b)] was more representative of bulk oxygen in-diffusion.

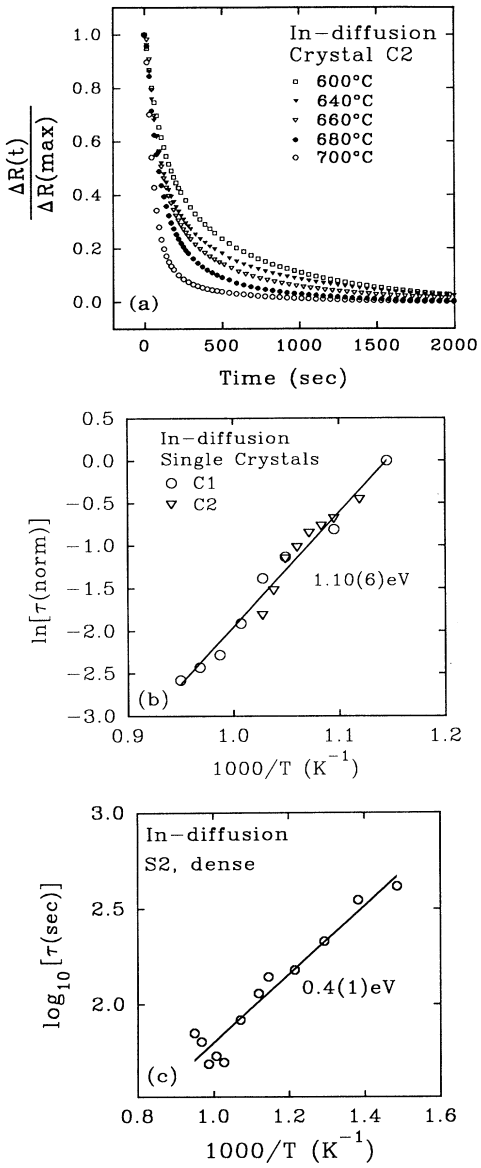

FIG. 2. (a) Normalized in-diffusion resistance isotherms from 600–700 °C in crystal *C*2 reveal a change in functional form with temperature. (b) An Arrhenius plot of normalized relaxation times for oxygen in-diffusion into *C*1 and *C*2 crystals suggests a single mechanism with an activation energy of 1.10(6) eV. (c) An Arrhenius plot of the relaxation times for oxygen in-diffusion into *dense,* coarse-grain polycrystalline specimen *S*2 from 400–780 °C. The low activation energy (0.4(1) eV) in comparison with single crystals (~1.10(6) eV) suggests that the formation of a highly oxygenated, highly conductive shell may mask intrinsic in-diffusion behavior.

B. Out-diffusion

The rate of resistance change during out-diffusion for the porous specimen *S*1 increased with temperature from

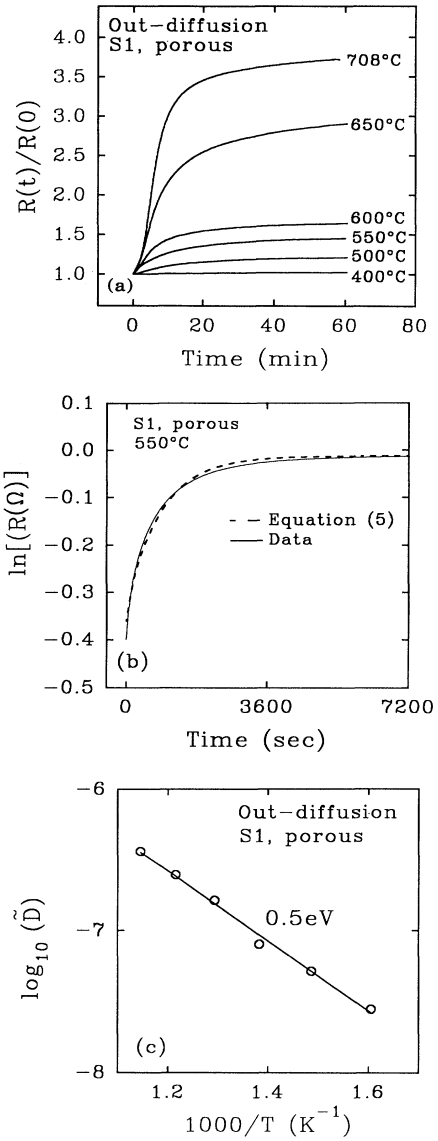

FIG. 3. (a) Resistance as a function of time for oxygen out-diffusion for *porous*, fine-grain specimen $S1$. (b) Resistance as a function of time for oxygen out-diffusion at 550 °C and the corresponding fit to Eq. (5). (c) Arrhenius plot of the chemical diffusivities for oxygen out-diffusion below 600 °C for the *porous*, fine-grain specimen $S1$. The diffusivities were estimated from Eq. (6) with an effective diffusion length equal to the specimen thickness ($L = 0.05$ cm).

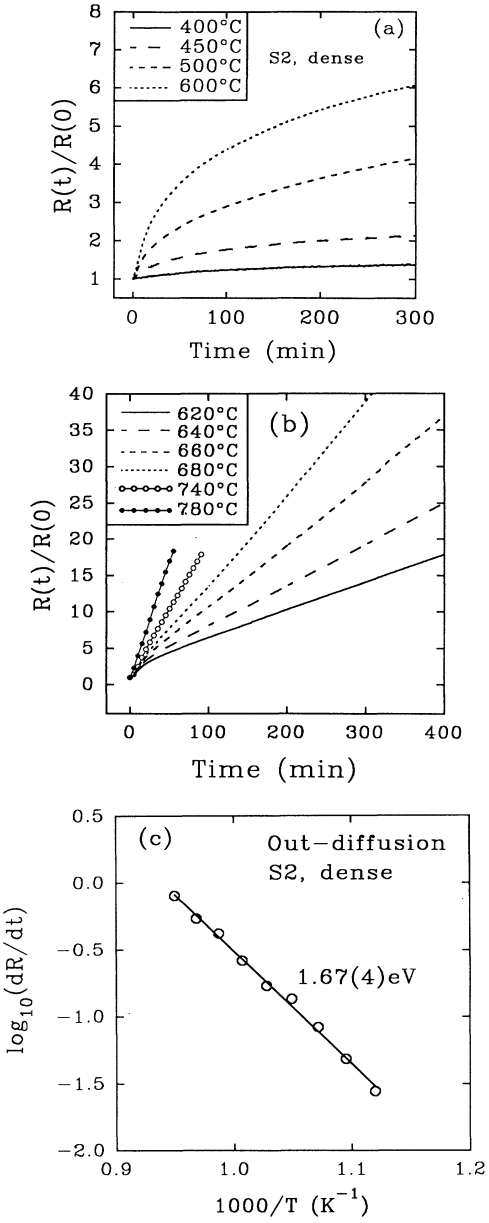

FIG. 4. Resistance increase during oxygen out-diffusion for *dense*, coarse-grain specimen $S2$ at temperatures (a) below 600 °C and (b) above 600 °C. There appears to be a crossover from diffusion-controlled to surface-limited out-diffusion behavior near 600 °C. (c) Temperature dependence of $\log_{10}(dR/dt)$ for oxygen out-diffusion for *dense*, coarse-grain specimen $S2$.

400–708 °C [Fig. 3(a)]. The resistance behavior was well described by a one-dimensional diffusion equation [Eq. (5)] [e.g., Fig. 3(b)]. The effective diffusion length L needed to accurately calculate $\tilde{D}$ [Eq. (6)] theoretically ranges from the average grain size to the external dimensions of the specimen depending on both porosity and the contribution of grain-boundary diffusion. As a first approximation, $\tilde{D}$ for $S1$ were estimated by using the thinnest sample dimension ($L \sim 0.05$ cm) as the effective diffusion length [Eq. (6)], which yielded an Arrhenius equation of the form

$$\tilde{D} = (2.6(5) \times 10^{-4}\ \text{cm}^2/\text{sec}) \exp\left[\frac{-0.5\ \text{eV}}{kT}\right] \qquad (7)$$

from 350–600 °C [Fig. 3(c)]. The connected porosity of specimen $S1$ in conjunction with the possibility of fast grain-boundary diffusion suggests that the average grain size could control the effective diffusion length. Howev-

TABLE II. Activation energies for oxygen diffusion in single-crystal and polycrystalline YBCO.

Specimen type	E (eV)	Temperature range	Comments[a]
Crystal $C1, C2$	1.10	600–780°C	ID
Polycrystal $S1$	0.5	350–600 °C	OD,GB,SE
(porous, 75%; 6 μm)			
Polycrystal $S2$	0.6	400–600 °C	OD,GB,SE
(dense, 95%; 19 μm)	1.67	600–780 °C	OD,SRC
	0.4	400–780 °C	ID,SE

[a]Key: OD (out-diffusion), ID (in-diffusion), SRC (surface-reaction controlled), GB (grain-boundary diffusion), SE (shell effects).

er, the Arrhenius expression obtained using $L=6$ μm (Table I) had a prefactor of 10^{-8} cm^2/sec, which was unreasonably small. The values of $\tilde{D}$ for $S1$ determined from Eq. (7) should, however, be interpreted as upper limits [Fig. 3(c)].

Out-diffusion curves for the dense, coarse-grain specimen $S2$ are shown in Figs. 4(a) and 4(b) both below and above 600 °C, respectively. The resistance increase accompanying out-diffusion was linear with time above 600 °C [Fig. 4(b)] but had exponential forms below 600 °C [Fig. 4(a)]. This suggests a crossover from diffusion-limited to surface reaction-limited diffusion near 600 °C during out-diffusion in an argon atmosphere. A similar crossover was observed during out-diffusion in argon for single crystals near 600 °C,[18] but not in porous specimens (e.g., $S1$). Below 600 °C, several days would have been required to obtain saturation resistances for the dense YBCO specimens (e.g., $S2$). Consequently, dense specimens were not completely deoxygenated below 600 °C, which precluded the calculation of reliable relaxation times. The activation energy, however, for out-diffusion for $S2$ was determined from a constant resistance cut made through Fig. 4(a) to obtain characteristic times τ' at each temperature. These were fit to the standard expression

$$\tau' = \tau'_0 \exp\left[\frac{E_0}{kT}\right] \tag{8}$$

yielding an activation energy of $E_0 = 0.6(1)$ eV (Table II). Within experimental error, this value was identical to the value (0.5(1) eV) obtained for the porous specimen $S1$ [Fig. 3(c)].

The activation energy for out-diffusion below 600 °C in both dense and porous polycrystalline specimens (0.5–0.6 eV) was lower than the activation energies for $\tilde{D}$ for crystals [e.g., Fig. 2(b)] and reported for oxygen tracer diffusion ($\sim$1 eV).[3–5] This suggests a high-diffusivity pathway such as grain boundaries or external surfaces. Evidence for grain-boundary diffusion was also observed in dynamic heating experiments with single-crystal and polycrystalline specimens.[13,16] The resistance behavior of orthorhombic YBCO ($x \approx 1$) was metallic and increased linearly with temperature in pure oxygen up to approximately 350 °C for polycrystalline ceramics[16] and up to 500 °C for single crystals.[13,16] Above these temperatures appreciable oxygen out-diffusion occurred and the resistance increased more rapidly. This suggests that near 350 °C grain-boundary diffusion becomes active in polycrystalline material, while significant bulk diffusion does not occur until close to 500 °C. Internal friction measurements[53] have observed a Debye-like damping peak near 530 °C, which was attributed to basal plane oxygen hopping at the onset of bulk lattice diffusion. The above discussion suggests that optimum oxygen incorporation will occur near 500 °C where appreciable lattice diffusion would lead to an equilibrium oxygen content of approximately 6.9 (Ref. 54). Below 500 °C, however, grain-boundary diffusion dominates and additional incorporation of oxygen into the bulk becomes extremely slow. This may explain the difficulty in achieving complete oxygenation (i.e., $x=1$) in YBCO especially in single crystals and in large dense polycrystalline specimens at reduced temperatures.

C. Surface-controlled out-diffusion

Above 600 °C, out-diffusion of oxygen in single-crystal and dense polycrystalline specimens was assumed to be surface-reaction limited as suggested by the linear change of resistance with time, dR/dt [e.g., Fig. 4(B)]. The rate of oxygen out-diffusion was directly proportional to the change in carrier concentration dR/dt, which enabled the activation energy for out-diffusion to be calculated from,[14,27]

$$\left[\frac{dR}{dt}\right] = B_0 \exp\left[\frac{-E_0}{kT}\right], \tag{9}$$

where B_0 is the preexponential factor and E_0 the activation energy. Analysis of linear out-diffusion isotherms (dR/dt) for dense polycrystalline specimen $S2$ [Fig. 4(b)] as a function of temperature from 600–780 °C yielded a single activation energy of 1.67(4) eV [Fig. 4(c)].

The linear resistance behavior during oxygen out-diffusion for single crystals[14] and for *dense* polycrystalline specimens above 600 °C [e.g., Fig. 4(b)] was similar to the behavior reported[27] below 440 °C in polycrystalline specimens. However, most electrical conductivity studies on polycrystalline material exhibit an exponential increase in resistance during oxygen out-diffusion typical of a standard diffusion controlled process [for example, Refs. 21, 23, 25, 28, 30, and Fig. 3(a)]. Linear out-diffusion behavior was observed in polycrystalline material with high bulk density and coarse-grain size [e.g., specimen $S2$; Fig. 4(b)] suggesting that connected porosity or fine-grain size

gives rise to the nonlinear out-diffusion behavior reported in other studies[21,23,25,28,30] and observed in specimen $S1$ above 600 °C [Fig. 3(a)].

At this point, it is important to consider extrinsic factors that might be responsible for the linear resistance behavior during oxygen out-diffusion. These include, (i) a surface impurity film formed during preparation or, (ii) phase decomposition at the surface during out-diffusion measurements. It has been suggested[4] that a surface film on YBCO samples, which develops during sample preparation, impedes oxygen exchange. However, in this study, the rectangular bars obtained from polycrystalline pellets were polished, and crystals were cut or fractured from much larger crystals, which exposed fresh (100)/(010) surfaces for oxygen exchange. Consequently, an impurity film formed during specimen synthesis was not responsible for the surface barrier for out-diffusion.

Phase decomposition (ii) at temperatures above 600 °C could have resulted in surface-reaction limited oxygen out-diffusion. There were, however, several observations that make this possibility unlikely. Linear resistance behavior was not observed during oxygen out-diffusion in the porous specimen, $S1$ [Fig. 3(a)], which by virtue of the larger internal and external surface area should make the material more susceptible to phase decomposition. Irreversible phase decomposition in $S1$ should lead to drift in the equilibrium resistance values $R(\infty)$ for repeated diffusion anneals. However, $R(\infty)$ in both polycrystalline and single-crystal specimens was always regained between successive diffusion runs suggesting that, if a secondary phase developed during out-diffusion in argon, it was thermodynamically reversible. A recent paper[55] suggested that the reversible formation of $YBa_2Cu_4O_8$ at the YBCO grain surface during out-diffusion gave rise to a surface barrier for out-diffusion. However, it is difficult to ascribe an explicable source for the additional Ba and Cu content. Also, $YBa_2Cu_4O_8$ formation is usually favored in high oxygen overpressures and should not form, while YBCO is undergoing reduction.

In addition, x-ray analysis, optical microscopy, and Auger analysis were used in an attempt to detect any surface phase present. X-ray diffraction did not detect impurity phases in any of the specimens even after numerous diffusion experiments. *In situ* observation of the (001) face of single crystals in an optical microscope did not reveal changes in features that may accompany phase decomposition during oxygen diffusion (e.g., tarnishing, pitting, etc.). In order to detect possible trace impurities, however, semiquantitative chemical analysis of YBCO crystal surfaces and near-surface composition was determined on a PHI model 660 Scanning Auger microscope, which could be operated in a sputter mode. Both (001) and (100/010) surfaces of as-grown crystals were found to have trace amounts of zirconia and carbon, which disappeared immediately upon sputtering. The Y-Ba-Cu-O ratio was essentially constant from the surface into the near-surface region. Crystal $C2$ was examined after one month of diffusion measurements and after an additional two months at 600 °C. The (001) surface was found to have slightly excess barium along with carbon and zirconium, however, the near surface region was entirely Y-Ba-Cu-O. The (100/010) surfaces were found to have more excess barium than the (001) surface, and carbon and zirconia were found to penetrate further into the near-surface region (<50 nm) before a constant Y-Ba-Cu-O ratio was obtained. As suggested by diffusion anisotropy, the (100/010) surfaces of a YBCO crystal were more reactive than the (001) surface during oxygen exchange. Although surface phases were not detected by x-ray analysis or observed by optical microscopy, Auger analysis detected trace impurities at the (100/010) surfaces of crystals.

D. Intrinsic diffusion rates: influence of microstructure

There is still some controversy surrounding the intrinsic rates of oxygen in-diffusion and out-diffusion in YBCO. Thermogravimetric analysis (TGA) has reported in-diffusion to be both faster[33] and equal[12] to out-diffusion. Most electrical-resistance studies, however, report *faster* in-diffusion than out-diffusion in polycrystalline material,[19,21,23,27] however, a study on single crystals reported *slower* in-diffusion than out-diffusion.[15] It is possible that the relative rates of in- and out-diffusion may depend on both the temperature of the measurement and the specimen's microstructure. A study[42] reported that the relative rates of in- and out-diffusion vary with temperature, becoming nearly identical at higher temperatures. Correspondingly, the influence of microstructure on the measured activation energies and chemical diffusivities was supported, for example, by a TGA study,[34] which reported the activation energy for oxygen diffusion to be greater for a polycrystalline pellet (~ 1.5 eV) than a loose powder (~ 1.2 eV). The reported discrepancies on diffusion rates in electrical-resistance measurements may also be due the formation of a highly oxygenated, highly conductive shell region during in-diffusion. The influence of a highly oxygenated shell will now be discussed with relation to its extrinsic effect on electrical-resistance measurements and its intrinsic effect on oxygen diffusion rates.

The influence of microstructure on the resistance behavior of YBCO during oxygen out- and in-diffusion is exemplified in Figs. 5 and 6. During out-diffusion in argon at 708 °C, the resistance of single-crystal $C1$ increased linearly with time typical of a surface-reaction controlled process [Fig. 5(a)]. Oxygen in-diffusion was initiated by exchange from argon to oxygen and was evident in the resulting resistance change, which first decreased rapidly and then more slowly with time [Fig. 5(a)]. If out-diffusion was driven to completion at 708 °C, it took more than 24 h for crystal $C1$ to reach a saturation resistance. Examination of dense polycrystalline YBCO [e.g., $S2$ in Fig. 1(c)], revealed that the resistance increase during out-diffusion was also linear [Fig. 5(c)] and, if taken to completion, saturated in ~ 24 h. Similar times for saturation for out-diffusion in crystal $C1$ and dense polycrystal $S2$, together with nearly identical effective diffusion lengths ($L \sim 0.9-1.0$ mm, Table I), suggests that oxygen out-diffusion in dense polycrystalline

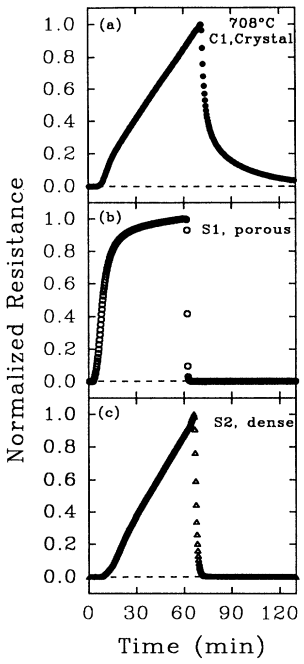

FIG. 5. Normalized resistance as a function of time for oxygen out-diffusion and in-diffusion at 708 °C for (a) single-crystal $C1$, (b) *porous,* fine-grain specimen $S1$, and (c) *dense,* coarse-grain specimen $S2$ (see Fig. 1). The resistance increased during oxygen out-diffusion and decreased for oxygen in-diffusion in all specimens, however, the functional forms are noticeably different. Note that in (a) the initial resistance was still not regained after a 1 h oxygen anneal, which suggests that oxygen in-diffusion was intrinsically slower than out-diffusion.

YBCO was not significantly affected by grain-boundary diffusion or shell effects. However, introducing connected porosity into YBCO [e.g., $S1$ in Fig. 1(b)] led to a non-linear increase in resistance during out-diffusion [Fig. 5(b)], which if driven to completion, saturated after

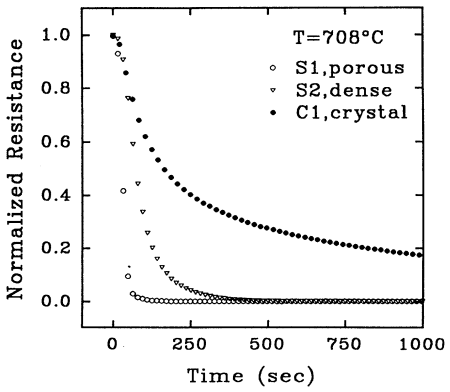

FIG. 6. Normalized resistance for oxygen in-diffusion at 708 °C in polycrystalline and single-crystal YBCO. The difference in functional form between *porous* $S1$ and *dense* $S2$ polycrystalline specimens suggests that grain size and/or bulk density influenced the in-diffusion kinetics.

~ 3 h. This nonlinear behavior, and rapid saturation in $S1$ in comparison with single crystals and dense polycrystalline $S2$, was attributed to the connected porosity in $S1$, which made more internal surface area available for oxygen exchange and, also, shortened the diffusion pathway, L.

Measurements on several single crystals indicated that the intrinsic rate of oxygen in-diffusion was comparable to, if not slower than, the rate of out-diffusion [e.g., Fig. 5(a)].[15] This was in contradiction to reports[19,21,23,27] for extremely fast in-diffusion for polycrystalline specimens [e.g., Figs. 5(b) and 5(c)]. As a means of illustrating these discrepancies, the resistance behavior during oxygen in-diffusion for $C1$, $S1$, and $S2$ (Fig. 5) are shown for smaller time increments in Fig. 6. A clear difference is seen in the rate of resistance decrease between porous and dense specimens indicating that connected porosity will, as expected, increase the rate of oxygen in-diffusion (Fig. 6). In addition, the equilibrium resistance $R(\infty)$ value upon oxygen in-diffusion was recovered more quickly for polycrystalline specimens compared with the crystal, which incorrectly suggests that oxygen in-diffusion was more rapid than out-diffusion [Figs. 5(b), 5(c), and 6].

The apparent rate of oxygen in-diffusion was more rapid in $S2$ in comparison with single-crystal $C1$ even though the effective diffusion lengths were similar (Fig. 6 and Table I). One possibility, for such apparently faster in-diffusion for $S2$ was that it had a greater surface area (approximately $100\times$) than the small crystal (Table I). In addition, oxygen exchange would occur primarily at the edges of a platelet single crystal due to the highly anisotropic D^*.[5] However, if the larger surface area for $S2$ was the only cause for rapid in-diffusion, then the rate of out-diffusion in $S2$ should have been, correspondingly, much faster than in crystal $C1$. The apparent rapid in-diffusion for $S2$ was therefore attributed to shell effects in which the formation of an initial highly oxygenated surface layer caused a short-circuit pathway for current flow. This gave a measured overall resistance that was not representative of the bulk oxygen content. Consequently, reports of faster in-diffusion than out-diffusion in polycrystalline YBCO, especially as determined from electrical-resistance measurements, are most likely due to extrinsic factors.[19,21,23,27]

There are several possibilities for the slow recovery of the equilibrium resistance $R(\infty)$ during in-diffusion in single crystals [e.g., Fig. 5(a)], including, (i) slow oxygen ordering kinetics, (ii) reversible phase decomposition and, (iii) slower in-diffusion than out-diffusion. The existence of a series of oxygen superlattice structures from $0.3 < x < 0.8$ (Ref. 56) and of room-temperature oxygen mobility[57–60] suggests that the effective hole density not only depends on the total oxygen content but also on the local coordination and ordering of oxygen.[61] Consequently, the slow recovery of $R(\infty)$ in Fig. 5(a) could be due to time-dependent ordering behavior (i). However, at high temperatures (e.g., $\gtrsim 600$ °C), the kinetics of oxygen ordering are expected to be rapid in comparison with the time scale of the diffusion measurement and should not greatly influence the effective carrier concentration. If reversible phase decomposition (ii) did occur during out-

diffusion in argon, then the slow recovery of the equilibrium resistance during in-diffusion may be due to the new phase slowly reverting back to YBCO. However, as discussed in Sec. III C, thermodynamically reversible phase decomposition (ii) appears to be unlikely.

The intrinsic rates of oxygen in- and out-diffusion (iii) were more clearly distinguished in single-crystal specimens [e.g., Fig. 5(a)]. The surface area to volume ratio for single crystals was much less than polycrystalline specimens, consequently, a highly conductive layer around a crystal's edge would have less of an effect on the overall resistance. Upon inspection of Fig. 5(a), the intrinsic rate of in-diffusion appears slower than out-diffusion for single crystals (iii). This type of behavior has been observed at all temperatures (600–780 °C) and for other crystals we have measured regardless of the length of the initial argon anneal. It is suggested that upon oxygenation, a crystal will quickly form a highly oxygenated layer around its edges, which coarsens with time, thus, leading to increasingly slower in-diffusion rates [e.g., Fig. 5(a)]. Oxygen diffusion through this layer would be hindered by several factors; a lower concentration of oxygen vacancies in comparison with the bulk; and, in the orthorhombic structure, ordered oxygen regions and twin boundaries. Both Monte Carlo simulations[62] and reported anisotropy in the tracer-diffusion coefficients[5] ($\tilde{D}_b \approx 100\tilde{D}_a$) suggests that ordered regions impede oxygen diffusion. In addition, the observation of an increasing chemical diffusivity $\tilde{D}$ with decreasing oxygen content at 708 °C (Ref. 17) is to be expected when in-diffusion is intrinsically slower than out-diffusion.[63]

Reports[19,21,23,27] of faster in-diffusion than out-diffusion by electrical-resistance measurements did not satisfactorily address the possibility that shell effects may lead to different apparent rates. As means of illustration, series and parallel resistor models for cubic grains can be used as a first approximation to illustrate the influence of time-varying heterogeneous oxygen concentration distributions on a sample's overall resistivity characteristics during oxygen exchange. The overall resistivity ρ_t of a sample during the initial stages of oxygen in-diffusion can be modeled by a parallel resistor network

$$\frac{1}{\rho_t} = \frac{1}{\rho_b} + \frac{2x_{gb}}{3\rho_{gb}} , \tag{10}$$

where ρ_b and ρ_{gb} are the resistivities of the bulk and of the shell, respectively, and x_{gb} the volume fraction of the shell for cubic grains. Likewise, a simple series model may describe out-diffusion:

$$\rho_t = \rho_b + \frac{x_{gb}\rho_{gb}}{3} . \tag{11}$$

At 700 °C, the resistivities of fully oxygenated and deoxygenated dense YBCO polycrystals were approximately 10 and 1000 mΩ cm, respectively. Consequently, during in-diffusion $\rho_{gb} = 10$ mΩ cm and $\rho_b = 1000$ mΩ cm, while during out-diffusion the values of ρ_{gb} and ρ_b were interchanged. Figure 7 shows the change in overall resistivity versus the effective thicknesses of shells x_{gb} of highly oxygenated and deoxygenated material during in- and out-diffusion, respectively. Even assuming that the rates of in- and out-diffusion are equal, there was a considerably more rapid decrease in resistivity during in-diffusion than a resistivity increase during out-diffusion. In other words, a *deoxygenated* shell formed during out-diffusion would have a lesser effect on the overall rate of resistance change in comparison to an equally thick *oxygenated* shell formed during in-diffusion. The influence of oxygen in- and out-diffusion on the resistance behavior in YBCO is probably more complex than described by Eqs. (10)–(11), however, these models serve as a simple illustration of how measurements of resistance characteristics during oxygen diffusion may lead to different apparent rates of oxidation and reduction.

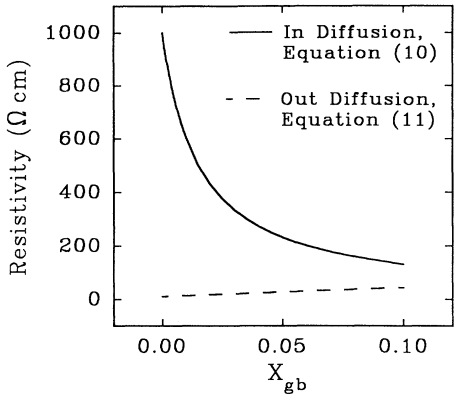

FIG. 7. The possible influence of heterogeneous oxygen distributions on the rate of resistance change for oxygen in- and out-diffusion as estimated from parallel and series resistor models [Eqs. (10) and (11)]. x_{gb} is the effective volume of the shell for cubic grains.

IV. CONCLUSION

In summary, the study of the time-dependent electrical characteristics of single-crystal and polycrystalline YBCO during oxygen in- and out-diffusion has allowed for intrinsic diffusion characteristics to be distinguished from those that are influenced by extrinsic microstructure effects. Diffusion rates and activation energies were found to be dependent on microstructure under certain conditions, which accounts for the many apparent discrepancies reported in the literature for chemical oxygen diffusion in YBCO superconductors. In-diffusion in dense YBCO specimens had an activation energy of 0.4 eV from 400–780 °C, while oxygen out-diffusion in dense and porous material had an activation energy of 0.5–0.6 eV below 600 °. These low energies, in comparison with those determined from tracer diffusivities (~1 eV) and from measurements on single crystals, suggests high-diffusivity pathways along internal surfaces (e.g., grain boundaries) or external surfaces. In addition, the rate of oxygen in-diffusion was observed to be comparable to, if not *slower,* than out-diffusion in single crystals of YBCO at all measurement temperatures (600–780 °C) with an activation energy of 1.10(6) eV.

The formation of a highly oxygenated shell during oxygen in-diffusion had two major effects on the electrical resistance of YBCO specimens. One, the shell behaved as a highly conductive, short-circuit pathway yielding resistances that were not representative of the bulk, particularly in polycrystalline specimens. This extrinsic effect made the rate of in-diffusion appear to be much faster than out-diffusion in polycrystalline specimens when first examined by resistance measurements. Simple parallel and series resistor models were used to illustrate this effect. Two, a highly oxygenated shell also behaves as a barrier to further oxygen in-diffusion. A lower concentration of oxygen vacancies and/or more ordered oxygen regions in this shell would make oxygen diffusion through the layer increasingly slower. The use of single-crystal specimens enabled the intrinsic effect of the diffusion barrier for the highly oxygenated shell region to be more clearly distinguished from the extrinsic effect of high-conductivity pathways.

ACKNOWLEDGMENTS

The authors greatly appreciate the assistance of their colleagues P. D. Han and A. Asthana, and the use of facilities in the Materials Research Laboratory at the University of Illinois. Auger analysis was carried out by Dr. Zhengkui Xu. The authors would also like to thank S. J. Rothman and J. L. Routbort for helpful discussions. The project was supported by the Air Force Office of Scientific Research, Grant No. URI-41318, through a University Research Initiative on Phase Transformations in Ceramics and by the National Science Foundation, Grant No. DMR 88-09854, through the Science and Technology Center for Superconductivity.

[1]R. J. Cava, A. W. Hewat, E. A. Hewat, B. Batlogg, M. Marezio, K. M. Rabe, J. J. Krajewski, W. F. Peck, and L. W. Rupp, Physica C **165**, 419 (1990).

[2]J. D. Jorgensen, B. W. Veal, A. P. Paulikas, L. J. Nowicki, G. W. Crabtree, H. Claus, and W. K. Kwok, Phys. Rev. B **41**, 1863 (1990).

[3]For a recent review, see S. J. Rothman and J. L. Routbort, in *Diffusion in Materials,* edited by A. L. Laskar *et al.* (Kluwer, Dordecht, 1990), p. 393.

[4]S. J. Rothman, J. L. Routbort, and J. E. Baker, Phys. Rev. B **40**, 8852 (1989).

[5]S. J. Rothman, J. L. Routbort, U. Welp, and J. E. Baker, Phys. Rev. B **44**, 2326 (1991).

[6]X. M. Xie, T. G. Chen, and J. Huang, Phys. Status Solidi A **110**, 415 (1988).

[7]X. M. Xie, T. G. Chen, and Z. L. Wu, Phys. Rev. B **40**, 4549 (1989).

[8]J. L. Tallon and M. P. Staines, J. Appl. Phys. **68**, 3998 (1990).

[9]G. Cannelli, R. Cantelli, F. Cordero, M. Ferretti, and F. Trequattrini, Solid State Commun. **77**, 429 (1991).

[10]P. G. Shewmon, *Diffusion in Solids* (Williams, Jenks, OK, 1983).

[11]P. Meuffels, R. Naeven, and H. Wenzl, Physica C **161**, 539 (1989).

[12]P. Kishio, K. Suzuki, T. Hasegawa, T. Yamamoto, K. Kitazawa, and K. Fueki, J. Solid State Chem. **82**, 192 (1989).

[13]J. R. LaGraff, P. D. Han, and D. A. Payne, Physica C **169**, 355 (1990).

[14]J. R. LaGraff, P. D. Han, and D. A. Payne, Phys. Rev. B **43**, 441 (1991).

[15]J. R. LaGraff, P. D. Han, and D. A. Payne, in *Defects in Materials,* edited by P. D. Bristowe, J. E. Epperson, J. E. Griffith, and Z. Liliental-Weber, MRS Symposia Proceedings No. 209 (Materials Research Society, Pittsburgh, 1991), p. 801.

[16]J. R. LaGraff and D. A. Payne, in *Physics and Materials Science of High-Temperature Superconductors II,* edited by R. Kossowsky, B. Raveau, and S. Patapis (Kluwer, Dordecht, 1992), pp. 225–246.

[17]J. R. LaGraff and D. A. Payne (unpublished).

[18]J. R. LaGraff, Ph.D. thesis, University of Illinois at Urbana-Champaign, 1992.

[19]K. N. Tu, S. I. Park, and C. C. Tsuei, Appl. Phys. Lett. **51**, 2158 (1987).

[20]S. I. Park, C. C. Tsuei, and K. N. Tu, Phys. Rev. B **37**, 2305 (1988).

[21]G. Sageev Grader, P. K. Gallagher, J. Thomson, and M. Gurvitch, Appl. Phys. A **45**, 179 (1988).

[22]K. N. Tu, C. C. Tsuei, S. K. Park, and A. Levi, Phys. Rev. B **38**, 772 (1988).

[23]J. Park, P. Kostic, and J. P. Singh, Mater. Lett. **6**, 393 (1988).

[24]K. N. Tu, N. C. Yeh, S. I. Park, and C. C. Tsuei, Phys. Rev. B **38**, 5118 (1988).

[25]A. T. Fiory, S. Martin, L. F. Schneemeyer, R. M. Fleming, A. E. White, and J. V. Waszczak, Phys. Rev. B **38**, 7129 (1988).

[26]N. C. Yeh, K. N. Tu, S. I. Park, and C. C. Tsuei, Phys. Rev. B **38**, 7087 (1988).

[27]K. N. Tu, N. C. Yeh, S. I. Park, and C. C. Tsuei, Phys. Rev. B **39**, 304 (1989).

[28]G. Ottaviani, C. Nobili, F. Nava, M. Affronte, T. Manfredini, F. C. Matacotta, and E. Galli, Phys. Rev. B **39**, 9069 (1989).

[29]Y. Song, X. D. Chen, J. R. Gaines, and J. W. Gilje, J. Mater. Res. **5**, 27 (1990).

[30]C. Nobili, G. Ottaviani, M. C. Rossi, and M. Sparpaglione, Physica C **168**, 549 (1990).

[31]K. Yamamoto, B. M. Lairson, J. C. Bravman, and T. H. Geballe, J. Appl. Phys. **69**, 7189 (1991).

[32]P. K. Gallagher, Adv. Ceram. Mater. **2**, 632 (1987).

[33]T. Umemura, K. Egawa, M. Wakata, and K. Yoshizaki, Jpn. J. Appl. Phys. **28**, L1945 (1989).

[34]L. T. Shi and K. N. Tu, Appl. Phys. Lett. **55**, 1351 (1989).

[35]Y. Zhao, T. Shi, S. Hu, and L. Xie, Mater. Lett. **8**, 83 (1989).

[36]T. B. Tang and W. Lo, Physica C **174**, 463 (1991).

[37]D. J. Vischjager, P. J. Van Der Put, J. Schram, and J. Schoonman, Solid State Ionics **27**, 199 (1988).

[38]E. J. M. O'Sullivan and B. P. Chang, Appl. Phys. Lett. **52**, 1441 (1988).

[39]J. MacManus, D. Fray, and J. Evetts, Physica C **162-164**, 143 (1989).

[40]Y. Scolnik, E. Sabatani, and D. Cahen, Physica C **174**, 273 (1991).

[41]J. MacManus, D. J. Fray, and J. E. Evetts, Physica C **190**, 511 (1992).

[42]E. Ruckenstein and A. K. Mallick, Mater. Lett. **7**, 122 (1988).

[43]H. F. Poulsen, N. H. Andersen, and B. Lebech, Physica C **173**, 387 (1991).

[44]S. Jantsch, J. Ihringer, J. K. Maichle, W. Prandl, S.

Kemmler-Sack, R. Kiemel, S. Losch, W. Schafer, M. Schlichenmaier, and A. W. Hewat, J. Less-Common. Met. **150**, 167 (1989).

[45]B. A. Glowacki, R. J. Highmore, K. F. Peters, A. L. Greer, and J. E. Evetts, Supercond. Sci. Technol. **1**, 7 (1988).

[46]H. Hermes, M. Forster, and H. E. Schaefer, Phys. Rev. B **43**, 10 399 (1991).

[47]J. Crank, *The Mathematics of Diffusion* (Clarendon, Oxford, 1975).

[48]J. R. LaGraff, E. C. Behrman, J. A. T. Taylor, F. J. Rotella, J. D. Jorgensen, L. Q. Wang, and P. G. Mattocks, Phys. Rev. B **39**, 347 (1989).

[49]H. C. Montgomery, J. Appl. Phys. **42**, 2971 (1971); L. J. van der Pauw, Philips Res. Rep. **16**, 187 (1961).

[50]For example, U. Welp, S. Fleshler, W. K. Kwok, J. Downey, Y. Fang, G. W. Crabtree, and J. Z. Liu, Phys. Rev. B **42**, 10 189 (1990); T. A. Friedmann, M. W. Rabin, J. Giapinzakis, J. P. Rice, and D. M. Ginsberg, Phys. Rev. B **42**, 6217 (1990); G. Sageev Grader, P. K. Gallagher, and E. M. Gyorgy, Appl. Phys. Lett. **51**, 1115 (1987); P. P. Freitas and T. S. Plaskett, Phys. Rev. B **36**, 5723 (1987).

[51]Y. Gao, K. L. Merkle, C. Zhang, U. Balachandran, and R. B. Poeppel, J. Mater. Res. **5**, 1363 (1990); W. K. Lee and A. S. Nowick, J. Mater. Res. **5**, 1855 (1990); E. A. Cooper, A. K. Gangopadhyay, T. T. Mason, and U. Balachandran, J. Mater. Res. **6**, 1393 (1991).

[52]J. R. LaGraff and D. A. Payne, Ferroelectrics **130**, 87 (1992).

[53]J. L. Tallon, A. H. Schuitema, and N. E. Tapp, Appl. Phys. Lett. **52**, 507 (1988).

[54]T. B. Lindemer, J. F. Hunley, J. E. Gates, A. L. Sutton, J. Brynestad, C. R. Hubbard, and P. K. Gallagher, J. Am. Ceram. Soc. **72**, 1775 (1989).

[55]L. T. Shi and K. N. Tu, Appl. Phys. Lett. **59**, 2040 (1991).

[56]R. Beyers, B. T. Ahn, G. Gorman, V. Y. Lee, S. S. P. Parkin, M. L. Ramirez, K. P. Roche, J. E. Vazquez, T. M. Gur, and R. A. Huggins, Nature (London) **340**, 619 (1989); D. de Fontaine, G. Ceder, and M. Asta, *ibid.* **343**, 544 (1990).

[57]I. Poberaj, D. Mihailovic, and S. Bernik, Phys. Rev. B **42**, 393 (1990).

[58]B. W. Veal, H. You, A. P. Paulikas, H. Shi, Y. Fang, and J. W. Downey, Phys. Rev. B **42**, 4770 (1990).

[59]B. W. Veal, A. P. Paulikas, H. You, H. Shi, Y. Fang, and J. W. Downey, Phys. Rev. B **42**, 6305 (1990).

[60]J. D. Jorgensen, S. Pei, P. Lightfoot, H. Shi, A. P. Paulikas, and B. W. Veal, Physica C **167**, 571 (1990).

[61]G. Cedar, R. McCormick and D. de Fontaine Phys. Rev. B **44**, 2377 (1991).

[62]J. V. Andersen, H. Bohr, and O. G. Mouritsen, Phys. Rev. B **42**, 283 (1990).

[63]J. Crank and M. E. Henry, Trans. Faraday Soc. **45**, 636 (1949).

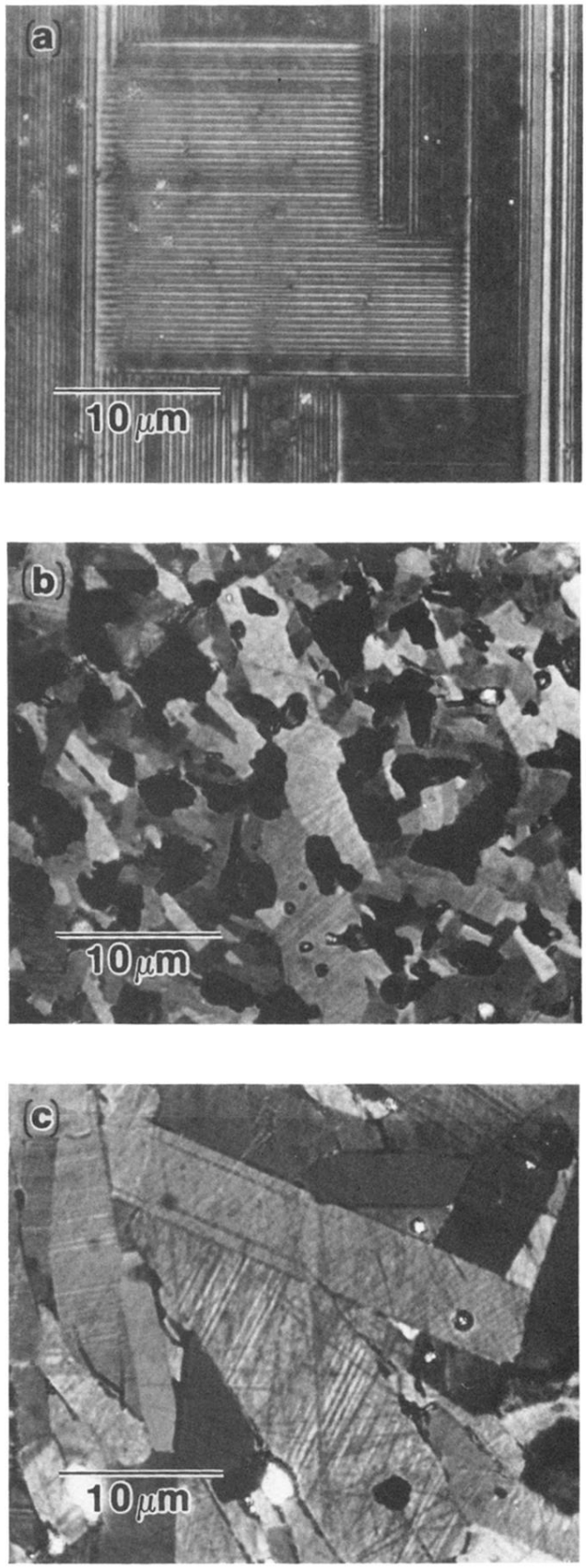

FIG. 1. Optical photomicrographs under cross-polarized reflected light of (a) single-crystal, (b) *porous,* fine-grain polycrystalline specimen $S1$, and (c) *dense,* coarse-grain polycrystalline specimen $S2$.